Letter

Study of the electromagnetic Dalitz decay $J/\psi \to e^+e^-\pi^0$

M. Ablikim *et al.*[*]
(BESIII Collaboration)

(Received 8 January 2025; accepted 2 July 2025; published 28 July 2025)

We report the first measurement of the dielectron invariant mass dependent transition form factor in the electromagnetic Dalitz decay $J/\psi \to e^+e^-\pi^0$ using $(10087 \pm 44) \times 10^6$ J/ψ events collected by the BESIII detector. A clear $\rho - \omega$ interference structure is observed, consistent with the pion form factor, which offers a novel approach to extract the hadronic vacuum polarization contribution to the anomalous muon magnetic moment (a_μ) and refine the predictions of the vector meson dominance (VMD) model and hadronic light-by-light contribution to a_μ. By taking into account the contribution of this $\rho - \omega$ interference structure, the branching fraction of $J/\psi \to e^+e^-\pi^0$ in the full e^+e^- invariant mass range is also measured for the first time to be $(8.06 \pm 0.31(\text{stat}) \pm 0.38(\text{syst})) \times 10^{-7}$, approximately twice the nonresonant VMD prediction.

DOI: 10.1103/yglh-sfbg

An electromagnetic (EM) Dalitz decay [1] proceeds via conversion of an off-shell photon into a lepton pair [2]. The q^2-dependent transition form factor (TFF), where q^2 is the four-momentum transfer squared and is equal to the square of the dilepton invariant mass [3], provides access to possible deviations from the standard pointlike prediction of quantum electrodynamics (QED) [2]. Thus, a TFF is a sensitive tool to probe the inner structure of the involved hadrons. Within the vector meson dominance (VMD) model [4], the TFF describes the interaction of the photons with hadrons via an intermediate vector meson V' in the timelike region [5]. These TFFs are important inputs in the calculation of the hadronic light-by-light contribution of the anomalous magnetic moment of the muon [6], $a_\mu = (g_\mu - 2)/2$, which is of great interest in precision tests of the Standard Model [7–9] and EM Dalitz decay rates [2].

Most measured EM Dalitz decays of the light unflavored vector mesons ρ, ω, and ϕ [10,11] are compatible with the VMD assumption [2]. However, some of the experimental results, such as $\omega \to \mu^+\mu^-\pi^0$, indicate large deviations [12,13] that are difficult to understand with existing theoretical models [14]. A similar situation has recently also appeared in the EM Dalitz decays of charmonium vector mesons, such as in recent measurements of the EM Dalitz decays $J/\psi \to e^+e^-P$ ($P = \pi^0, \eta, \eta'$) [15,16]. The measured branching fractions of $J/\psi \to e^+e^-\eta/\eta'$ agree well with the VMD prediction [17], which does not include the contributions of intermediate V' resonances. We refer to this as the nonresonant VMD prediction. However, the branching fraction of $J/\psi \to e^+e^-\pi^0$, $(7.56 \pm 1.32 \pm 0.50) \times 10^{-7}$ [15], measured by BESIII for dielectron invariant masses ($m_{e^+e^-}$) less than 0.4 GeV/c^2 using 225 million J/ψ events, deviates by more than three standard deviations from the predictions based on the nonresonant VMD prediction [17], an effective Lagrangian-based analysis [18], Khuri-Treiman (KT) analysis [19], and dispersion theory [20]. The latter three models [18–20] also take into account the contribution of the intermediate light vector meson ρ. This discrepancy may disappear after considering the resonant contributions from the isospin conserving decay $J/\psi \to \rho\pi^0$ and the isospin violating decays $J/\psi \to \omega/\phi\pi^0$ [21]. However, the well-known $\rho - \omega$ interference, as proposed by Glashow [22], may also appear in these decays, as discussed in Ref. [23].

An experimental study of $\rho - \omega$ interference is essential for testing charge symmetry violation (CSV) [24–26], QCD sum rules (QCDSR) [27,28], chiral perturbation theory (ChPT) [29,30], and hidden local symmetry (HLS) models [31,32]. This interference has been well established in the pionic cross section $\sigma(e^+e^- \to \pi^+\pi^-)$ [33–35], and impacts the measurements of the isospin-violating $\omega \to \pi^+\pi^-$ decay rate [33], the running QED coupling [36], the 2π contribution to the hadronic vacuum polarization (HVP) in a_μ [33–35], as well as tests of isospin violation in asymmetric nuclear matter [37] and lattice QCD benchmarks [38]. In particular, the observed $\rho - \omega$ interference provides essential input for constraining isospin-breaking and QED corrections in lattice QCD [38,39], understanding

[*]Full author list given at the end of the article.

Published by the American Physical Society under the terms of the Creative Commons Attribution 4.0 International license. Further distribution of this work must maintain attribution to the author(s) and the published article's title, journal citation, and DOI. Funded by SCOAP[3].

CSV in nuclear forces [24–26], and modeling vector meson properties in nuclear matter and hot, dense QCD environments such as the quark-gluon plasma [40].

An investigation of $\rho-\omega$ interference in a purely EM channel was previously reported via the photoproduction of electron-positron pairs off carbon [41], beryllium [42], and hydrogen [43] targets, but the phases of the interference were found to be different from those corresponding to pionic channels, such as $e^+e^-\to\pi^+\pi^-$ [33–35]. This discrepancy may be resolved by investigating the $\rho-\omega$ interference in the intermediate resonances of $J/\psi\to e^+e^-\pi^0$. The same J/ψ decay also tests various theoretical models [2,17–20], could improve the accuracy of $J/\psi\to V'\pi^0$ ($V'=\rho,\ \omega$) decay rates [21], and probes G-parity violation [23]. This paper reports the first measurement of the q^2-dependent TFF and an improved measurement of the branching fraction of the EM Dalitz decay $J/\psi\to e^+e^-\pi^0$ in the full $m_{e^+e^-}$ spectrum using a data sample of $(10\,087\pm 44)\times 10^6$ J/ψ events collected by the BESIII detector.

BESIII is a general purpose detector operating at the e^+e^- BEPCII collider, and is described in more detail in Ref. [44]. Monte Carlo (MC) simulated events based on Geant4 [45] are used to study the detection efficiency, to optimize the event selection criteria, and to investigate potential backgrounds. Time-dependent effects, such as beam-related backgrounds and detector running conditions during the data collection period, are included in the MC simulation. An inclusive MC sample of 10 billion events of generic J/ψ decays, generated by EvtGen [46] for known decay modes with branching fractions quoted in Ref. [21] and by LUNDCHARM [47] for unknown decay modes, is used for background studies. The signal MC sample is generated using EvtGen [46] according to a Lorentz-invariant amplitude [48], where the TFF function is directly extracted from the data while taking into account the contribution of intermediate V' resonances in the decay as described below. Furthermore, another signal MC sample containing only the nonresonant contribution of the $J/\psi\to e^+e^-\pi^0$ decay is also generated with the same model by setting the TFF to unity. This is also referred to as the pointlike process and is used to optimize the event selection criteria and study the $m_{e^+e^-}$ dependent TFF.

We select events of interest by requiring two oppositely charged tracks and at least two good photon candidates. Charged tracks are reconstructed from the ionization signals measured by the main drift chamber (MDC). The point of closest approach of each charged track to the e^+e^- interaction point (IP) is required to be within ± 10.0 cm along the beam direction, which is the symmetry axis of the MDC and within ± 1.0 cm in the plane perpendicular to the beam. Each charged track is required to be within the active region of the MDC $|\cos\theta|<0.93$, where θ is the polar angle with respect to the positron beam along the z-axis. The particle identification (PID) algorithm, based on the specific energy loss dE/dx and information from the time-of-flight (TOF) system and the electromagnetic calorimeter (EMC), forms a likelihood $\mathcal{L}(h)$, where h is a particle hypothesis of $e^\pm$, $\pi^\pm$ or $K^\pm$ charged tracks. One of the charged tracks is identified as e^- and the other as e^+ by requiring $\mathcal{L}(e^\pm)>\mathcal{L}(\pi^\pm)$ and $\mathcal{L}(e^\pm)>\mathcal{L}(K^\pm)$. We further suppress pion contamination by requiring $E/p_{e^\pm}>0.8\ c$ for those charged tracks with momenta larger than $0.25\ \mathrm{GeV}/c$, where E is the energy deposited in the EMC and $p_{e^\pm}$ is the momentum measured by the MDC.

Showers are reconstructed from clusters of energy deposited in the EMC crystals. The shower energy of each photon is required to be greater than 25 MeV in the barrel region ($|\cos\theta|<0.8$) or 50 MeV in the end-cap regions ($0.86<|\cos\theta|<0.92$). In order to improve the reconstruction efficiency and energy resolution, the energy deposited in the nearby TOF is taken into account. Showers poorly reconstructed in the transition region between the barrel and end-cap are discarded. In order to suppress the electronic noise and energy deposition unrelated to the events, the photon time as given by the EMC is required to be less than 700 ns after the collision.

A vertex fit is performed to the two charged tracks to ensure that they originate from a common vertex point. In order to improve the π^0 mass resolution, a four-constraint (4C) kinematic fit imposing energy and momentum conservation is implemented for the selected charged tracks and the two good photon candidates under the hypothesis of $J/\psi\to e^+e^-\gamma\gamma$. If there are more than two good photon candidates in the event, all $\gamma\gamma$ combinations are tested and the pair that gives the lowest value of chi-square of the kinematic fit, $\chi^2_{4\mathrm{C}}$, is selected. To suppress peaking background from $J/\psi\to\gamma\pi^0\pi^0$, where one of the π^0 candidates decays in its Dalitz decay mode $\pi^0\to\gamma e^+e^-$, the $\chi^2_{4\mathrm{C}}$ is further required to be less than 100. Candidate events are required to have a diphoton invariant mass, $m_{\gamma\gamma}$, within the range $[0.09, 0.18]\ \mathrm{GeV}/c^2$.

The MC studies indicate that the background is dominated by the radiative Bhabha process $e^+e^-\to\gamma e^+e^-$, especially in the high $m_{e^+e^-}$ region, due to its large cross section. The background contributes a smooth distribution in the $m_{\gamma\gamma}$ spectrum. This nonpeaking background is suppressed by requiring the momentum of the selected $e^\pm$ to be less than $1.45\ \mathrm{GeV}/c$ and the energy of the low energy photon (E_{γ_2}) used to reconstruct the π^0 candidate to be larger than 0.14 GeV.

At this stage, the peaking background in $m_{\gamma\gamma}$ spectrum is dominated by events from the radiative decay $J/\psi\to\gamma\pi^0$, in which the radiative photon converts into an e^+e^- pair in the detector material. The distance from the vertex point of the e^+e^- pair to the origin in the x-y plane is defined as $\delta_{xy}=\sqrt{R_x^2+R_y^2}$, where R_x and R_y are the coordinates of the reconstructed vertex point along the x and y directions, respectively, as described in Ref. [49]. In the distribution of R_y versus R_x, the signal events from $J/\psi\to e^+e^-\pi^0$

accumulate in the center of the circle, and the background events from $J/\psi \to \gamma\pi^0$ accumulate in the circles with radii of 3.5 cm and 6.5 cm corresponding to the positions of the beam pipe and inner wall of the MDC, respectively, as described in Fig. 1 of Ref. [50]. A requirement of $\delta_{xy} < 2$ cm is imposed, which eliminates around 98% of the γ conversion background with a loss of about 20% of the signal events.

The two-photon process [51], which proceeds via the interaction of two virtual photons emitted by the lepton pair in an e^+e^- collider experiment, can produce an even C-parity state of the pseudoscalar meson. In the case of π^0 production, the corresponding process $e^+e^- \to e^+e^-\pi^0$ has the same final state as the signal of interest. It therefore contributes as a peaking background in the $m_{\gamma\gamma}$ spectrum. An independent sample of $\psi(3770)$ data with an integrated luminosity of 2.93 fb^{-1} [34], which is away from J/ψ resonance and is assumed to provide a pure sample of $e^+e^- \to e^+e^-\pi^0$ events, is used to study this background. The two-photon background events mainly accumulate in the bands of $\cos\theta(e^+) > 0.8$ or $\cos\theta(e^-) < -0.8$, away from the signal that accumulates around $\cos\theta(e^+) = \cos\theta(e^-)$, as described in Ref. [52]. This background is suppressed by requiring $\cos\theta(e^+) < 0.8$ and $\cos\theta(e^-) > -0.8$. After applying this selection criterion, the number of two-photon events in the J/ψ data sample is evaluated as $N_{J/\psi} = f \cdot N_{\psi(3770)}$, where $N_{\psi(3770)}$ is the number of signal events in the $\psi(3770)$ data sample surviving the same selection criteria, and $f = \frac{\mathcal{L}_{J/\psi}}{\mathcal{L}_{\psi(3770)}} \cdot \frac{\sigma_{J/\psi}}{\sigma_{\psi(3770)}} \cdot \frac{\epsilon_{J/\psi}}{\epsilon_{\psi(3770)}} = 3.59 \pm 0.02$ is the scale factor between the two data samples X ($X = J/\psi$ and $\psi(3770)$), which takes into account the integrated luminosities $\mathcal{L}_X$, the cross sections σ_X and the efficiencies ϵ_X [51]. The detection efficiency ratio $\frac{\epsilon_{J/\psi}}{\epsilon_{\psi(3770)}}$ and cross-section ratio $\frac{\sigma_{J/\psi}}{\sigma_{\psi(3770)}}$ are evaluated to be 4.03 ± 0.02 and 0.878 ± 0.001, respectively, with the EKHARA generator [53]. The value of $\epsilon_{\psi(3770)}$ is reduced due to the selection criteria on the $e^\pm$ momentum, as described above. The yield $N_{\psi(3770)} = 27.9 \pm 13.6$ is obtained by performing an extended maximum likelihood (ML) fit to the $m_{\gamma\gamma}$ spectrum of events selected from the $\psi(3770)$ data sample. Therefore, the expected number of two-photon events for the J/ψ data sample is estimated to be 100.0 ± 48.8.

Figure 1 shows the $m_{e^+e^-}$ distribution for surviving events from the data, signal MC, and the remaining background processes. The contribution from the nonpeaking background is dominated by the radiative Bhabha process. This background is evaluated using events in the π^0 sideband regions, defined as [0.02, 0.08] and $[0.19, 0.30]$ GeV/c^2. The peaking background is dominated by the decay $J/\psi \to \pi^+\pi^-\pi^0$ (99.4 ± 3.8 events including the ρ resonance and due to the $\pi^\pm$ mis-identified to be $e^\pm$), $J/\psi \to \gamma\pi^0$ (35.2 ± 1.7 events), $J/\psi \to \gamma\pi^0\pi^0$ (2.8 ± 0.2 events), and $J/\psi \to \omega\pi^0$, $\omega \to \pi^+\pi^-$ (0.5 ± 0.1 events), where uncertainties include statistical and systematic uncertainties. The expected numbers of background events are evaluated using large MC samples normalized to their corresponding branching fractions quoted from Ref. [21]. The simulated events are also used for evaluating the resonant contributions of $J/\psi \to V'\pi^0$, $V' \to e^+e^-$, considered to be part of the signal mode, and are 690.0 ± 86.6 events for $\rho \to e^+e^-$ and 85.5 ± 9.8 for $\omega \to e^+e^-$, normalized to the branching fractions in Ref. [21].

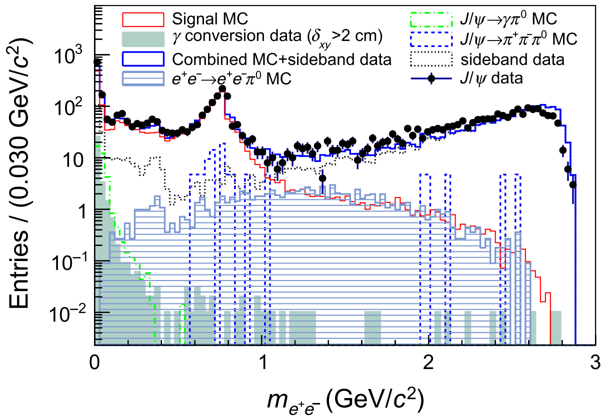

FIG. 1. Distribution of $m_{e^+e^-}$ for selected events in data (black dots with error bars), signal MC (red histogram), $J/\psi \to \gamma\pi^0$ MC (green long-dashed dotted histogram), where γ converts in material, γ conversion data (sky green), $J/\psi \to \pi^+\pi^-\pi^0$ (blue dashed histogram), sideband data (black dotted histogram), two-photon process MC (gray blue pattern) and combined MC and sideband data (solid blue histogram). The signal MC sample includes the contributions of both resonant and nonresonant components from $J/\psi \to e^+e^-\pi^0$. The γ conversion data were obtained from the events with $\delta_{xy} > 2$ cm [50].

The signal yield is determined by performing an extended ML fit to the $m_{\gamma\gamma}$ spectrum of the selected candidate events in data. In the fit, the probability density function (PDF) of the signal is described by the MC simulated shape convolved with a Gaussian function (with free parameters), which compensates for the resolution difference between data and MC simulation. The PDF of the nonpeaking background is described by a first-order Chebyshev polynomial function with free parameters. The fit is shown in Fig. 2 over the full $m_{e^+e^-}$ spectrum, and yields $N_{\rm sig}^{\rm data} = 2347 \pm 66$ events, including both signal and peaking background contributions. By subtracting the contributions from the decays $J/\psi \to \pi^+\pi^-\pi^0$, $J/\psi \to \gamma\pi^0$, $J/\psi \to \gamma\pi^0\pi^0$, $J/\psi \to \omega(\to \pi^+\pi^-)\pi^0$, $J/\psi \to \omega\pi^0\pi^0$, and the two-photon process $e^+e^- \to e^+e^-\pi^0$, estimated above, the net signal yield is determined to be $N_{\rm sig} = 2108.9 \pm 82.2$, where the total uncertainties on the peaking backgrounds are added in quadrature with the statistical uncertainty on $N_{\rm sig}$. The obtained $N_{\rm sig}$ includes the contributions of the nonresonant $J/\psi \to e^+e^-\pi^0$ and the

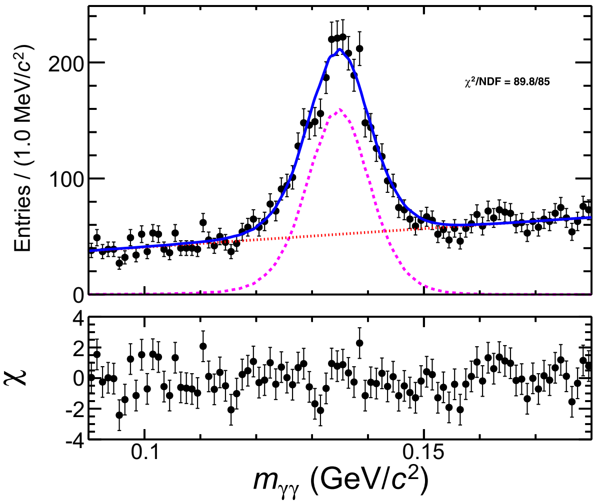

FIG. 2. The fit to the $m_{\gamma\gamma}$ distribution (top) together with the normalized fit residuals (bottom). The p value of the fit is 0.34. The black dots with error bars are data, the pink dashed curve the signal, the red dotted curve the nonpeaking background, and the blue solid curve the total projection.

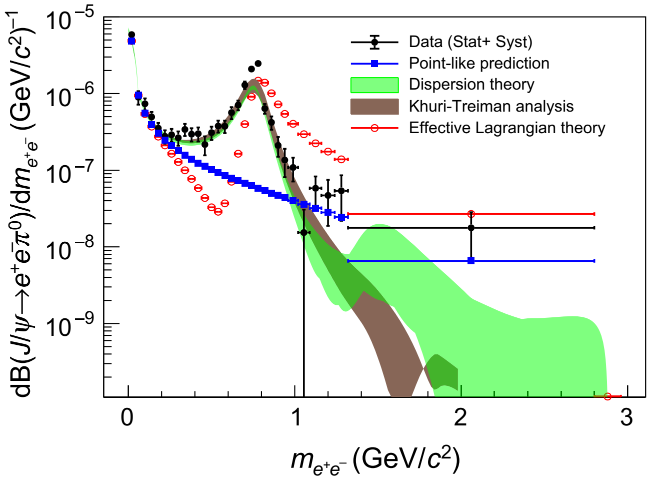

FIG. 3. The differential branching fraction for $J/\psi \to e^+e^-\pi^0$ normalized to the bin size versus $m_{e^+e^-}$ for data (black dots with error bars, including the statistical and systematic uncertainties combined in quadrature), the pointlike prediction (blue squares with error bars), the effective Lagrangian theory prediction [18] (red circles with error bars), KT analysis [19] (brown band), and the dispersion theory [20] prediction (green band).

resonant $J/\psi \to \rho/\omega\pi^0$, $\rho/\omega \to e^+e^-$ decays. The branching fraction of $J/\psi \to e^+e^-\pi^0$ is calculated to be $(8.06 \pm 0.31 \pm 0.38) \times 10^{-7}$, where the first uncertainty is statistical and the second is systematic as described below and in the Supplemental Material [50], by the following formula,

$$\mathcal{B}(J/\psi \to e^+e^-\pi^0) = \frac{N_{\rm sig}}{N_{J/\psi} \cdot \epsilon \cdot \mathcal{B}(\pi^0 \to \gamma\gamma)}. \quad (1)$$

Here, $\epsilon = 26.3\%$ is the signal selection efficiency obtained from a signal MC sample, depicted in Fig. 1, generated using the fitted TFF function of Eq. (2) with a pole mass $\Lambda = 3.686\ \mathrm{GeV}/c^2$, as described below to take into account both the resonant and nonresonant contributions of $J/\psi \to e^+e^-\pi^0$. The $\mathcal{B}(\pi^0 \to \gamma\gamma)$ is the branching fraction of $\pi^0 \to \gamma\gamma$ from Ref. [21] and $N_{J/\psi} = (10\,087 \pm 44) \times 10^6$ is the total number of J/ψ events from Ref. [54].

To avoid the observed ρ/ω contributions, the branching fraction of $J/\psi \to e^+e^-\pi^0$ for $m_{e^+e^-} < 0.3\ \mathrm{GeV}/c^2$ is determined to be $(4.41 \pm 0.18 \pm 0.21) \times 10^{-7}$, which is consistent with the nonresonant VMD prediction from Ref. [17], using a similar fit procedure detailed in Ref. [50]. The observed deviation from the nonresonant VMD prediction [17], which was larger in the previous BESIII measurement [15], disappears with a large J/ψ data sample. However, our analysis reveals that nonresonant VMD prediction [17] underestimates the total branching fraction by approximately a factor of two, as it does not include contributions from the ρ/ω resonances.

The q^2-dependent TFF of $J/\psi \to e^+e^-$ is studied by comparing the measured differential branching fraction to that of the pointlike prediction. The signal yield in each $m_{e^+e^-}$ bin is extracted by the same ML fit on the $m_{\gamma\gamma}$ distribution as described above. The corresponding detection efficiency (ϵ) is calculated with a signal MC sample generated under the pointlike assumption that the TFF is equal to unity. In order to handle background from radiative Bhabha events, the fit is performed with various $m_{e^+e^-}$ bin widths with a total of 30 $m_{e^+e^-}$ points detailed in Table 1 of Ref. [50]. The obtained distribution of the differential branching fractions, calculated after subtracting the aforementioned peaking backgrounds (except the background from the two-photon process) using the signal yields in each bin of $m_{e^+e^-}$, deviates from the pointlike model prediction derived from the formula in Eq. (3.4) of Ref. [2], as well as from the effective Lagrangian-based analysis [18], KT analysis [19], and dispersion theory [20], as shown in Fig. 3. An interference between the ρ and ω is observed for the first time in the $J/\psi \to e^+e^-\pi^0$ decay. This behavior differs from that observed in previous measurements via the photoproduction of electron-positron pairs [41–43]. This difference arises from the isospin dynamics involved in the decays $J/\psi \to \rho\pi^0$ and $J/\psi \to \omega\pi^0$ [23].

The TFF ($|F_{J/\psi\pi^0}(q^2)|^2$) in each $m_{e^+e^-}$ bin, shown in Table 1 of Ref. [50], is calculated as the ratio of the corrected signal yield to the prediction of the pointlike model integrated over the $m_{e^+e^-}$ bin interval, as shown in Fig. 4. To achieve a unity value of the TFF at $q^2 = 0$, the $|F_{J/\psi\pi^0}(q^2)|^2$ versus $m_{e^+e^-}$ data are normalized using the central value of the TFF from the first $m_{e^+e^-}$ bin.

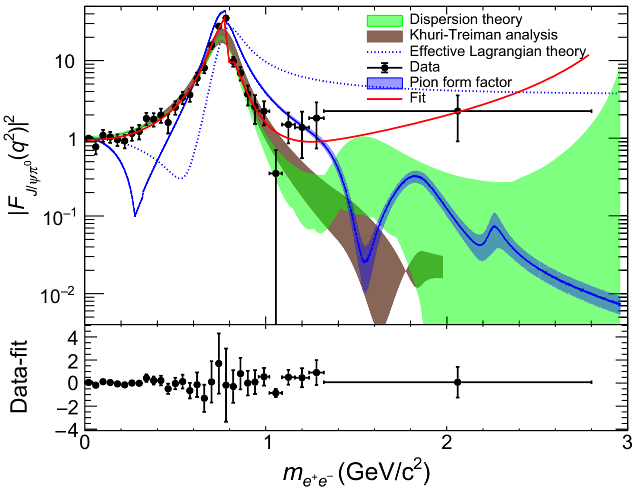

FIG. 4. Top: fit to the TFF versus $m_{e^+e^-}$ in data and (bottom) their fit residual values in each bin. The p value of the fit is 0.82. The black dots with error bars are data, which include both statistical and systematic uncertainties as described in the text and Ref. [50], the blue dotted curve comes from the effective Lagrangian theory [18], the brown and green bands come from the KT analysis [19], and dispersion theory [20], respectively, blue band is the pion form factor taken from the *BABAR* measurement [35] and the solid red curve is the fit result, which excludes the higher-order ρ resonances.

To study the observed $\rho-\omega$ interference, the TFF is fitted with the following combined function:

$$F_{J/\psi\pi^0}(q^2) = F^{\mathrm{GS}}_{J/\psi\pi^0}(q^2) + A_\Lambda \frac{1.}{1-q^2/\Lambda^2}, \qquad (2)$$

where $A_\Lambda = |A_\Lambda|e^{i\phi_\Lambda}$ is an amplitude with phase angle ϕ_Λ, and $F^{\mathrm{GS}}_{J/\psi\pi^0}(q^2)$ includes the contributions of both ρ resonances, which as described by a Gounaris-Sakurai function [55], and ω resonance, described by a Breit-Wigner function. The $F^{\mathrm{GS}}_{J/\psi\pi^0}(q^2)$ is given by the formula in Eq. (26) of Ref. [35] and has previously used by both the BESIII [34] and *BABAR* [35] experiments in the measurement of the $e^+e^- \to \pi^+\pi^-$ cross section in the ρ/ω mass region. The contributions of the ρ', ρ'', and ρ''' resonances are excluded in the fit.

Due to limited statistics, the mass and width of the ω meson are fixed to their world-average values [21], while the other parameters are left free during the fit. The obtained fit reveals that the observed $\rho-\omega$ interference pattern in the $J/\psi \to e^+e^-\pi^0$ TFF closely resembles the pattern seen in the $e^+e^- \to \pi^+\pi^-$ cross-section measurements in the ρ/ω mass region [33–35], offering an alternative approach to extract the HVP contribution to a_μ. The observed relatively narrow ρ resonance in data arises due to the electron mass, which accounts for the threshold effect in the low-mass region, as well as the interference between resonant and nonresonant processes in $J/\psi \to e^+e^-\pi^0$, as described in Ref. [50]. The fit yields the Λ value of 3.3 ± 0.7 GeV$/c^2$, which appears to be consistent with being above the combined mass threshold of $m_{J/\psi\pi^0}$. However, the uncertainty on this fitted value is quite large, limited by statistics in the high $m_{e^+e^-}$ region. Therefore, the fitted TFF function of Eq. (2) with $\Lambda = 3.686$ GeV$/c^2$ is used to generate the signal MC events for efficiency determination, as mentioned above. To properly account for the HVP contribution to a_μ, we perform an additional fit including higher order ρ resonances in the mass range $[2m_e, 1.28]$ GeV$/c^2$. Details are provided in Ref. [50].

According to Eq. (1), the systematic uncertainty associated with the branching fraction and TFF measurements include those from N_{sig}, the number of J/ψ events, reconstruction efficiencies, and secondary branching fractions, details of which are described in Ref. [50]. The systematic uncertainty is dominated by the signal model (0.6%), nonpeaking background PDF (2.2%), tracking efficiency (2.4%), PID (1.2%), photon reconstruction efficiency (0.4%), and $E/p_{e^\pm}$ (2.4%). Total systematic uncertainties for the branching fraction and TFF measurements are determined to be 4.7% and 6.6%, respectively, by adding the individual ones in quadrature.

In summary, using a data sample of $(10\,087 \pm 44) \times 10^6$ J/ψ events collected by the BESIII detector, we measure the TFF of $J/\psi \to e^+e^-\pi^0$ as a function of $m_{e^+e^-}$ for the first time. A clear $\rho-\omega$ interference pattern is observed, which closely matches that of the pionic form factor [33–35]. This result demonstrates the feasibility of probing isospin-violating effects and provides essential input for improving the VMD model [17] and the HLBL contribution to a_μ [7–9]. Furthermore, the observed $\rho-\omega$ interference offers a new way to extract the HVP contribution to a_μ [33–35]. After taking into account the contribution of this resonant structure, the branching fraction of $J/\psi \to e^+e^-\pi^0$ is measured for the first time in the full $m_{e^+e^-}$ spectrum, to be $(8.06 \pm 0.31(\mathrm{stat}) \pm 0.38(\mathrm{syst})) \times 10^{-7}$, approximately double the nonresonant VMD prediction [17]. These results can be measured with significantly improved precision at future facilities, such as the Super Tau-Charm Factory experiment [56].

Acknowledgments. The authors thank Bastian Kubis, Sergi Gonzalez-Solis, and Zhi-Hui Guo for providing the data for their theoretical predictions. The BESIII Collaboration thanks the staff of BEPCII and the IHEP computing center for their strong support. This work is supported in part by National Key R&D Program of China under Contracts No. 2020YFA0406300, No. 2020YFA0406400, No. 2023YFA1606000; National Natural Science Foundation of China (NSFC) under Contracts No. 11635010, No. 11735014, No. 11705192, No. 11935015, No. 11935016, No. 11935018, No. 11950410506, No. 12025502, No. 12035009, No. 12035013, No. 12061131003, No. 12192260, No. 12192261, No. 12192262, No. 12192263, No. 12192264, No. 12192265, No. 12221005, No. 12225509, No. 12235017, No. 12361141819; the Chinese Academy of Sciences (CAS) Large-Scale Scientific Facility Program; the CAS Center for Excellence in Particle Physics (CCEPP); Joint Large-Scale Scientific Facility Funds of the NSFC and CAS under Contract No. U1832207; 100 Talents Program of CAS; The Institute of Nuclear and Particle Physics (INPAC) and Shanghai Key Laboratory for Particle Physics and Cosmology; German Research Foundation DFG under Contracts No. 455635585, No. FOR5327, No. GRK 2149; Istituto Nazionale di Fisica Nucleare, Italy; Ministry of Development of Turkey under Contract No. DPT2006K-120470; National Research Foundation of Korea under Contract No. NRF-2022R1A2C1092335; National Science and Technology fund of Mongolia; National Science Research and Innovation Fund (NSRF) via the Program Management Unit for Human Resources & Institutional Development, Research and Innovation of Thailand under Contract No. B16F640076; Polish National Science Centre under Contract No. 2019/35/O/ST2/02907; The Chilean National Agency for Research and Development ANID PIA/APOYO AFB230003 and ANID FONDECYT regular 1230987; The Swedish Research Council; U.S. Department of Energy under Contract No. DE-FG02-05ER41374.

Data availability. The data are not publicly available. The data are available from the authors upon reasonable request.

[1] R. H. Dalitz, Proc. Phys. Soc. London Sect. A **64**, 667 (1951).
[2] L. G. Landsberg, Phys. Rep. **128**, 301 (1985).
[3] N. M. Kroll and W. Wada, Phys. Rev. **98**, 1355 (1955).
[4] J. J. Sakurai, *Currents and Mesons* (University of Chicago Press, Chicago, USA, 1969).
[5] V. M. Budnev and V. A. Karnakov, Pis'ma Zh. Eksp. Teor. Fiz. **29**, 439 (1979) [JETP Lett. **29**, 398 (1979)], http://jetpletters.ru/ps/1453/article_22116.pdf.
[6] G. Colangelo, M. Hoferichter, B. Kubis, M. Procura, and P. Stoffer, Phys. Lett. B **738**, 6 (2014); G. Colangelo, M. Hoferichter, M. Procura, and P. Stoffer, J. High Energy Phys. 09 (2015) 074.
[7] F. Jegerlehner and A. Nyffeler, Phys. Rep. **477**, 1 (2009).
[8] A. Nyffeler, Phys. Rev. D **94**, 053006 (2016).
[9] T. Aoyama, N. Asmussen, M. Benayoun *et al.*, Phys. Rep. **887**, 1 (2020); G. Colangelo, M. Davier, A. X. El-Khadra *et al.*, arXiv:2203.15810; B. Abi *et al.* (Muon $g-2$ Collaboration), Phys. Rev. Lett. **126**, 141801 (2021).
[10] M. Hoferichter, B. Kubis, S. Leupold, F. Niecknig, and S. P. Schneider, Eur. Phys. J. C **74**, 3180 (2014).
[11] C. Hanhart, A. Kupsc, U.-G. Meißner, F. Stollenwerk, and A. Wirzba, Eur. Phys. J. C **73**, 2668 (2013).
[12] R. Arnaldi *et al.* (NA60 Collaboration), Phys. Lett. B **677**, 260 (2009).
[13] G. Usai (NA60 Collaboration), Nucl. Phys. **A855**, 189 (2011).
[14] B. Ananthanarayan, I. Caprini, and B. Kubis, Eur. Phys. J. C **74**, 3209 (2014).
[15] M. Ablikim *et al.* (BESIII Collaboration), Phys. Rev. D **89**, 092008 (2014).
[16] M. Ablikim *et al.* (BESIII Collaboration), Phys. Rev. D **99**, 012006 (2019); **104**, 099901(E) (2021).
[17] J. Fu, H. B. Li, X. Qin, and M. Z. Yang, Mod. Phys. Lett. A **27**, 1250223 (2012).
[18] Y. H. Chen, Z. H. Guo, and B. S. Zhou, Phys. Rev. D **91**, 014010 (2015); L. W. Yan, Y. H. Chen, C. G. Duan, and Z. H. Guo, Phys. Rev. D **107**, 034022 (2023).
[19] M. Albaladejo *et al.* (JPAC Collaboration), Phys. Rev. D **108**, 014035 (2023).
[20] B. Kubis and F. Niecknig, Phys. Rev. D **91**, 036004 (2015).
[21] R. L. Workman *et al.* (Particle Data Group), Prog. Theor. Exp. Phys. **2022**, 083C01 (2022) and 2023.
[22] S. L. Glashow, Phys. Rev. Lett. **7**, 469 (1961).
[23] W. Dong, B. Yong, and Li Gang, Chin. Phys. C **38**, 063101 (2014).
[24] P. C. McNamee, M. D. Scadron, and S. A. Coon, Nucl. Phys. **A249**, 483 (1975).
[25] A. W. Thomas and K. Saito, arXiv:nucl-th/9507010; H. B. O'Connell, B. C. Pearce, A. W. Thomas, and A. G. Williams, Prog. Part. Nucl. Phys. **39**, 201 (1997).
[26] T. Goldman, J. Henderson, Jr., and A. Thomas, Few-Body Syst. **12**, 123 (1992).
[27] M. Shifman, A. Vainshtein, and V. Zakharov, Nucl. Phys. **B147**, 519 (1979).
[28] K. Maltman, Phys. Rev. D **53**, 2563 (1996).
[29] R. Urech, Phys. Lett. B **355**, 308 (1995).
[30] J. Bijnens, arXiv:hep-ph/9502393.
[31] M. Benayoun, P. David, L. DelBuono, and O. Leitner, Eur. Phys. J. C **65**, 211 (2010); M. Benayoun, P. David, L. DelBuono, O. Leitner, and H. B. O'Connell, Eur. Phys. J. C **55**, 199 (2008).
[32] M. Benayoun and H. O'Connell, Eur. Phys. J. C **22**, 503 (2001).
[33] F. V. Ignatov *et al.* (CMD-3 Collaboration), arXiv:2302.0883.
[34] M. Ablikim *et al.* (BESIII Collaboration), Phys. Lett. B **753**, 629 (2016).
[35] J. P. Lees *et al.* (*BABAR* Collaboration), Phys. Rev. D **86**, 032013 (2012).

[36] A. Anastasi *et al.* (KLOE-2 Collaboration), Phys. Lett. B **767**, 485 (2017).
[37] A. D. Mazumder, R. Hofmann, and M. Pospelov, Phys. Rev. C **63**, 015204 (2000).
[38] H. Yan, M. Mai, M. Garofalo, U.-G. Meißner, C. Liu, L. Liu, and C. Urbach, Phys. Rev. Lett. **133**, 211906 (2024).
[39] P. Boyle *et al.*, J. High Energy Phys. 02 (2023) 242.
[40] R. Rapp, Adv. High Energy Phys. **2013**, 148253 (2013).
[41] P. J. Biggs, D. W. Braben, R. W. Clifft, E. Gabathuler, P. Kitching, and R. E. Rand, Phys. Rev. Lett. **24**, 1197 (1970).
[42] H. Alvensleben *et al.*, Nucl. Phys. **B25**, 333 (1971).
[43] C. Djalali, M. Paolone, D. Weygand, and M. Wood, Proc. Sci. Hadron2013 (**2013**) 176.
[44] M. Ablikim *et al.* (BESIII Collaboration), Nucl. Instrum. Methods Phys. Res., Sect. A **614**, 345 (2010).
[45] S. Agostinelli *et al.* (GEANT4 Collaboration), Nucl. Instrum. Methods Phys. Res., Sect. A **506**, 250 (2003).
[46] D. J. Lange, Nucl. Instrum. Methods Phys. Res., Sect. A **462**, 152 (2001); R. G. Ping, Chin. Phys. C **32**, 599 (2008).
[47] J. C. Chen, G. Huang, X. Qi, D. Zhang, and Y. Zhu, Phys. Rev. D **62**, 034003 (2000).
[48] L. M. Gu, H. B. Li, X. X. Ma, and M. Z. Yang, Phys. Rev. D **100**, 016018 (2019).
[49] Z. R. Xu and K. L. He, Chin. Phys. C **36**, 742 (2012).
[50] See Supplemental Material at http://link.aps.org/supplemental/10.1103/yglh-sfbg for details on the γ conversion backgrounds, nonresonant contributions, systematic uncertainties, a table of the TFF determined in this work, and alternative TFF fit results.
[51] J. M. Bian *et al.*, Int. J. Mod. Phys. A **24**, 267 (2009).
[52] M. Ablikim *et al.* (BESIII Collaboration), Phys. Lett. B **783**, 452 (2018).
[53] H. Czyz, S. Ivashyn, A. Korchin, and O. Shekhovtsova, Phys. Rev. D **85**, 094010 (2012).
[54] M. Ablikim *et al.* (BESIII Collaboration), Chin. Phys. C **46**, 074001 (2022).
[55] G. J. Gounaris and J. J. Sakurai, Phys. Rev. Lett. **21**, 244 (1968).
[56] M. Achasov *et al.*, Front. Phys. **19**, 14701 (2024).

M. Ablikim,[1] M. N. Achasov,[4,c] P. Adlarson,[76] O. Afedulidis,[3] X. C. Ai,[81] R. Aliberti,[35] A. Amoroso,[75a,75c] Q. An,[72,58,a] Y. Bai,[57] O. Bakina,[36] I. Balossino,[29a] Y. Ban,[46,h] H.-R. Bao,[64] V. Batozskaya,[1,44] K. Begzsuren,[32] N. Berger,[35] M. Berlowski,[44] M. Bertani,[28a] D. Bettoni,[29a] F. Bianchi,[75a,75c] E. Bianco,[75a,75c] A. Bortone,[75a,75c] I. Boyko,[36] R. A. Briere,[5] A. Brueggemann,[69] H. Cai,[77] X. Cai,[1,58] A. Calcaterra,[28a] G. F. Cao,[1,64] N. Cao,[1,64] S. A. Cetin,[62a] J. F. Chang,[1,58] G. R. Che,[43] G. Chelkov,[36,b] C. Chen,[43] C. H. Chen,[9] Chao Chen,[55] G. Chen,[1] H. S. Chen,[1,64] H. Y. Chen,[20] M. L. Chen,[1,58,64] S. J. Chen,[42] S. L. Chen,[45] S. M. Chen,[61] T. Chen,[1,64] X. R. Chen,[31,64] X. T. Chen,[1,64] Y. B. Chen,[1,58] Y. Q. Chen,[34] Z. J. Chen,[25,i] Z. Y. Chen,[1,64] S. K. Choi,[10] G. Cibinetto,[29a] F. Cossio,[75c] J. J. Cui,[50] H. L. Dai,[1,58] J. P. Dai,[79] A. Dbeyssi,[18] R. E. de Boer,[3] D. Dedovich,[36] C. Q. Deng,[73] Z. Y. Deng,[1] A. Denig,[35] I. Denysenko,[36] M. Destefanis,[75a,75c] F. De Mori,[75a,75c] B. Ding,[67,1] X. X. Ding,[46,h] Y. Ding,[40] Y. Ding,[34] J. Dong,[1,58] L. Y. Dong,[1,64] M. Y. Dong,[1,58,64] X. Dong,[77] M. C. Du,[1] S. X. Du,[81] Y. Y. Duan,[55] Z. H. Duan,[42] P. Egorov,[36,b] Y. H. Fan,[45] J. Fang,[59] J. Fang,[1,58] S. S. Fang,[1,64] W. X. Fang,[1] Y. Fang,[1] Y. Q. Fang,[1,58] R. Farinelli,[29a] L. Fava,[75b,75c] F. Feldbauer,[3] G. Felici,[28a] C. Q. Feng,[72,58] J. H. Feng,[59] Y. T. Feng,[72,58] M. Fritsch,[3] C. D. Fu,[1] J. L. Fu,[64] Y. W. Fu,[1,64] H. Gao,[64] X. B. Gao,[41] Y. N. Gao,[46,h] Yang Gao,[72,58] S. Garbolino,[75c] I. Garzia,[29a,29b] L. Ge,[81] P. T. Ge,[19] Z. W. Ge,[42] C. Geng,[59] E. M. Gersabeck,[68] A. Gilman,[70] K. Goetzen,[13] L. Gong,[40] W. X. Gong,[1,58] W. Gradl,[35] S. Gramigna,[29a,29b] M. Greco,[75a,75c] M. H. Gu,[1,58] Y. T. Gu,[15] C. Y. Guan,[1,64] A. Q. Guo,[31,64] L. B. Guo,[41] M. J. Guo,[50] R. P. Guo,[49] Y. P. Guo,[12,g] A. Guskov,[36,b] J. Gutierrez,[27] K. L. Han,[64] T. T. Han,[1] F. Hanisch,[3] X. Q. Hao,[19] F. A. Harris,[66] K. K. He,[55] K. L. He,[1,64] F. H. Heinsius,[3] C. H. Heinz,[35] Y. K. Heng,[1,58,64] C. Herold,[60] T. Holtmann,[3] P. C. Hong,[34] G. Y. Hou,[1,64] X. T. Hou,[1,64] Y. R. Hou,[64] Z. L. Hou,[1] B. Y. Hu,[59] H. M. Hu,[1,64] J. F. Hu,[56,j] S. L. Hu,[12,g] T. Hu,[1,58,64] Y. Hu,[1] G. S. Huang,[72,58] K. X. Huang,[59] L. Q. Huang,[31,64] X. T. Huang,[50] Y. P. Huang,[1] Y. S. Huang,[59] T. Hussain,[74] F. Hölzken,[3] N. Hüsken,[35] N. in der Wiesche,[69] J. Jackson,[27] S. Janchiv,[32] J. H. Jeong,[10] Q. Ji,[1] Q. P. Ji,[19] W. Ji,[1,64] X. B. Ji,[1,64] X. L. Ji,[1,58] Y. Y. Ji,[50] X. Q. Jia,[50] Z. K. Jia,[72,58] D. Jiang,[1,64] H. B. Jiang,[77] P. C. Jiang,[46,h] S. S. Jiang,[39] T. J. Jiang,[16] X. S. Jiang,[1,58,64] Y. Jiang,[64] J. B. Jiao,[50] J. K. Jiao,[34] Z. Jiao,[23] S. Jin,[42] Y. Jin,[67] M. Q. Jing,[1,64] X. M. Jing,[64] T. Johansson,[76] S. Kabana,[33] N. Kalantar-Nayestanaki,[65] X. L. Kang,[9] X. S. Kang,[40] M. Kavatsyuk,[65] B. C. Ke,[81] V. Khachatryan,[27] A. Khoukaz,[69] R. Kiuchi,[1] O. B. Kolcu,[62a] B. Kopf,[3] M. Kuessner,[3] X. Kui,[1,64] N. Kumar,[26] A. Kupsc,[44,76] W. Kühn,[37] J. J. Lane,[68] L. Lavezzi,[75a,75c] T. T. Lei,[72,58] Z. H. Lei,[72,58] M. Lellmann,[35] T. Lenz,[35] C. Li,[47] C. Li,[43] C. H. Li,[39] Cheng Li,[72,58] D. M. Li,[81] F. Li,[1,58] G. Li,[1] H. B. Li,[1,64] H. J. Li,[19] H. N. Li,[56,j] Hui Li,[43] J. R. Li,[61] J. S. Li,[59] K. Li,[1] K. L. Li,[19] L. J. Li,[1,64] L. K. Li,[1] Lei Li,[48] M. H. Li,[43] P. R. Li,[38,k,l] Q. M. Li,[1,64] Q. X. Li,[50] R. Li,[17,31] S. X. Li,[12] T. Li,[50] W. D. Li,[1,64] W. G. Li,[1,a] X. Li,[1,64] X. H. Li,[72,58] X. L. Li,[50] X. Y. Li,[1,64] X. Z. Li,[59] Y. G. Li,[46,h] Z. J. Li,[59] Z. Y. Li,[79] C. Liang,[42] H. Liang,[1,64] H. Liang,[72,58] Y. F. Liang,[54] Y. T. Liang,[31,64] G. R. Liao,[14] Y. P. Liao,[1,64] J. Libby,[26] A. Limphirat,[60] C. C. Lin,[55] D. X. Lin,[31,64] T. Lin,[1] B. J. Liu,[1] B. X. Liu,[77] C. Liu,[34] C. X. Liu,[1] F. Liu,[1] F. H. Liu,[53] Feng Liu,[6] G. M. Liu,[56,j] H. Liu,[38,k,l] H. B. Liu,[15] H. H. Liu,[1] H. M. Liu,[1,64] Huihui Liu,[21] J. B. Liu,[72,58] J. Y. Liu,[1,64] K. Liu,[38,k,l] K. Y. Liu,[40] Ke Liu,[22] L. Liu,[72,58] L. C. Liu,[43] Lu Liu,[43] M. H. Liu,[12,g] P. L. Liu,[1] Q. Liu,[64] S. B. Liu,[72,58] T. Liu,[12,g] W. K. Liu,[43] W. M. Liu,[72,58] X. Liu,[38,k,l] X. Liu,[39] Y. Liu,[81] Y. Liu,[38,k,l] Y. B. Liu,[43] Z. A. Liu,[1,58,64] Z. D. Liu,[9] Z. Q. Liu,[50] X. C. Lou,[1,58,64] F. X. Lu,[59] H. J. Lu,[23] J. G. Lu,[1,58] X. L. Lu,[1] Y. Lu,[7] Y. P. Lu,[1,58] Z. H. Lu,[1,64] C. L. Luo,[41] J. R. Luo,[59] M. X. Luo,[80] T. Luo,[12,g] X. L. Luo,[1,58] X. R. Lyu,[64] Y. F. Lyu,[43] F. C. Ma,[40] H. Ma,[79] H. L. Ma,[1] J. L. Ma,[1,64] L. L. Ma,[50] L. R. Ma,[67] M. M. Ma,[1,64] Q. M. Ma,[1] R. Q. Ma,[1,64] T. Ma,[72,58] X. T. Ma,[1,64] X. Y. Ma,[1,58] Y. Ma,[46,h] Y. M. Ma,[31] F. E. Maas,[18] M. Maggiora,[75a,75c] S. Malde,[70] Y. J. Mao,[46,h] Z. P. Mao,[1] S. Marcello,[75a,75c] Z. X. Meng,[67] J. G. Messchendorp,[13,65] G. Mezzadri,[29a] H. Miao,[1,64] T. J. Min,[42] R. E. Mitchell,[27] X. H. Mo,[1,58,64] B. Moses,[27] N. Yu. Muchnoi,[4,c] J. Muskalla,[35] Y. Nefedov,[36] F. Nerling,[18,e] L. S. Nie,[20] I. B. Nikolaev,[4,c] Z. Ning,[1,58] S. Nisar,[11,m] Q. L. Niu,[38,k,l] W. D. Niu,[55] Y. Niu,[50] S. L. Olsen,[64] Q. Ouyang,[1,58,64] S. Pacetti,[28b,28c] X. Pan,[55] Y. Pan,[57] A. Pathak,[34] Y. P. Pei,[72,58] M. Pelizaeus,[3] H. P. Peng,[72,58] Y. Y. Peng,[38,k,l] K. Peters,[13,e] J. L. Ping,[41] R. G. Ping,[1,64] S. Plura,[35] V. Prasad,[33] F. Z. Qi,[1] H. Qi,[72,58] H. R. Qi,[61] M. Qi,[42] T. Y. Qi,[12,g] S. Qian,[1,58] W. B. Qian,[64] C. F. Qiao,[64] X. K. Qiao,[81] J. J. Qin,[73] L. Q. Qin,[14] L. Y. Qin,[72,58] X. P. Qin,[12,g] X. S. Qin,[50] Z. H. Qin,[1,58] J. F. Qiu,[1] Z. H. Qu,[73] C. F. Redmer,[35] K. J. Ren,[39] A. Rivetti,[75c] M. Rolo,[75c] G. Rong,[1,64] Ch. Rosner,[18] S. N. Ruan,[43] N. Salone,[44] A. Sarantsev,[36,d] Y. Schelhaas,[35] K. Schoenning,[76] M. Scodeggio,[29a] K. Y. Shan,[12,g] W. Shan,[24] X. Y. Shan,[72,58] Z. J. Shang,[38,k,l] J. F. Shangguan,[16] L. G. Shao,[1,64] M. Shao,[72,58] C. P. Shen,[12,g] H. F. Shen,[1,8] W. H. Shen,[64] X. Y. Shen,[1,64] B. A. Shi,[64] H. Shi,[72,58] H. C. Shi,[72,58] J. L. Shi,[12,g] J. Y. Shi,[1] Q. Q. Shi,[55] S. Y. Shi,[73] X. Shi,[1,58] J. J. Song,[19] T. Z. Song,[59] W. M. Song,[34,1] Y. J. Song,[12,g] Y. X. Song,[46,h,n] S. Sosio,[75a,75c] S. Spataro,[75a,75c] F. Stieler,[35] S. S. Su,[40] Y. J. Su,[64] G. B. Sun,[77] G. X. Sun,[1] H. Sun,[64] H. K. Sun,[1] J. F. Sun,[19] K. Sun,[61] L. Sun,[77] S. S. Sun,[1,64] T. Sun,[51,f] W. Y. Sun,[34] Y. Sun,[9] Y. J. Sun,[72,58] Y. Z. Sun,[1] Z. Q. Sun,[1,64] Z. T. Sun,[50] C. J. Tang,[54] G. Y. Tang,[1] J. Tang,[59] M. Tang,[72,58] Y. A. Tang,[77] L. Y. Tao,[73] Q. T. Tao,[25,i] M. Tat,[70] J. X. Teng,[72,58] V. Thoren,[76] W. H. Tian,[59] Y. Tian,[31,64] Z. F. Tian,[77] I. Uman,[62b] Y. Wan,[55] S. J. Wang,[50] B. Wang,[1] B. L. Wang,[64] Bo Wang,[72,58] D. Y. Wang,[46,h] F. Wang,[73] H. J. Wang,[38,k,l] J. J. Wang,[77] J. P. Wang,[50] K. Wang,[1,58] L. L. Wang,[1] M. Wang,[50] N. Y. Wang,[64] S. Wang,[12,g] S. Wang,[38,k,l] T. Wang,[12,g] T. J. Wang,[43] W. Wang,[73] W. Wang,[59] W. P. Wang,[35,58,72,o] X. Wang,[46,h] X. F. Wang,[38,k,l] X. J. Wang,[39] X. L. Wang,[12,g] X. N. Wang,[1] Y. Wang,[61] Y. D. Wang,[45] Y. F. Wang,[1,58,64] Y. L. Wang,[19] Y. N. Wang,[45] Y. Q. Wang,[1] Yaqian Wang,[17] Yi Wang,[61] Z. Wang,[1,58] Z. L. Wang,[73] Z. Y. Wang,[1,64] Ziyi Wang,[64] D. H. Wei,[14] F. Weidner,[69] S. P. Wen,[1] Y. R. Wen,[39] U. Wiedner,[3] G. Wilkinson,[70] M. Wolke,[76] L. Wollenberg,[3] C. Wu,[39] J. F. Wu,[1,8] L. H. Wu,[1] L. J. Wu,[1,64] X. Wu,[12,g] X. H. Wu,[34] Y. Wu,[72,58] Y. H. Wu,[55] Y. J. Wu,[31] Z. Wu,[1,58] L. Xia,[72,58] X. M. Xian,[39] B. H. Xiang,[1,64] T. Xiang,[46,h] D. Xiao,[38,k,l] G. Y. Xiao,[42] S. Y. Xiao,[1] Y. L. Xiao,[12,g] Z. J. Xiao,[41] C. Xie,[42] X. H. Xie,[46,h] Y. Xie,[50] Y. G. Xie,[1,58] Y. H. Xie,[6] Z. P. Xie,[72,58] T. Y. Xing,[1,64] C. F. Xu,[1,64] C. J. Xu,[59] G. F. Xu,[1] H. Y. Xu,[67,2,p] M. Xu,[72,58] Q. J. Xu,[16] Q. N. Xu,[30] W. Xu,[1] W. L. Xu,[67] X. P. Xu,[55] Y. Xu,[40] Y. C. Xu,[78] Z. S. Xu,[64] F. Yan,[12,g] L. Yan,[12,g] W. B. Yan,[72,58] W. C. Yan,[81] X. Q. Yan,[1,64] H. J. Yang,[51,f] H. L. Yang,[34] H. X. Yang,[1] T. Yang,[1] Y. Yang,[12,g] Y. F. Yang,[43] Y. F. Yang,[1,64] Y. X. Yang,[1,64] Z. W. Yang,[38,k,l] Z. P. Yao,[50] M. Ye,[1,58] M. H. Ye,[8] J. H. Yin,[1] Junhao Yin,[43] Z. Y. You,[59] B. X. Yu,[1,58,64] C. X. Yu,[43] G. Yu,[1,64] J. S. Yu,[25,i] M. C. Yu,[40] T. Yu,[73] X. D. Yu,[46,h] Y. C. Yu,[81] C. Z. Yuan,[1,64] J. Yuan,[34] J. Yuan,[45] L. Yuan,[2] S. C. Yuan,[1,64] Y. Yuan,[1,64] Z. Y. Yuan,[59] C. X. Yue,[39] A. A. Zafar,[74] F. R. Zeng,[50] S. H. Zeng,[63,o] X. Zeng,[12,g] Y. Zeng,[25,i] Y. J. Zeng,[59] Y. J. Zeng,[1,64] X. Y. Zhai,[34] Y. C. Zhai,[50] Y. H. Zhan,[59] A. Q. Zhang,[1,64] B. L. Zhang,[1,64] B. X. Zhang,[1] D. H. Zhang,[43] G. Y. Zhang,[19] H. Zhang,[72,58] H. Zhang,[81] H. C. Zhang,[1,58,64] H. H. Zhang,[59] H. H. Zhang,[34] H. Q. Zhang,[1,58,64] H. R. Zhang,[72,58] H. Y. Zhang,[1,58] J. Zhang,[81] J. Zhang,[59] J. J. Zhang,[52] J. L. Zhang,[20] J. Q. Zhang,[41] J. S. Zhang,[12,g] J. W. Zhang,[1,58,64] J. X. Zhang,[38,k,l] J. Y. Zhang,[1] J. Z. Zhang,[1,64] Jianyu Zhang,[64] L. M. Zhang,[61] Lei Zhang,[42] P. Zhang,[1,64] Q. Y. Zhang,[34] R. Y. Zhang,[38,k,l] S. H. Zhang,[1,64] Shulei Zhang,[25,i] X. D. Zhang,[45] X. M. Zhang,[1] X. Y. Zhang,[40] X. Y. Zhang,[50] Y. Zhang,[73] Y. Zhang,[1] Y. T. Zhang,[81] Y. H. Zhang,[1,58] Y. M. Zhang,[39] Yan Zhang,[72,58] Z. D. Zhang,[1] Z. H. Zhang,[1] Z. L. Zhang,[34] Z. Y. Zhang,[77] Z. Y. Zhang,[43] Z. Z. Zhang,[45] G. Zhao,[1] J. Y. Zhao,[1,64] J. Z. Zhao,[1,58] L. Zhao,[1] Lei Zhao,[72,58] M. G. Zhao,[43] N. Zhao,[79] R. P. Zhao,[64] S. J. Zhao,[81] Y. B. Zhao,[1,58] Y. X. Zhao,[31,64] Z. G. Zhao,[72,58] A. Zhemchugov,[36,b] B. Zheng,[73] B. M. Zheng,[34] J. P. Zheng,[1,58] W. J. Zheng,[1,64] Y. H. Zheng,[64] B. Zhong,[41] X. Zhong,[59] H. Zhou,[50] J. Y. Zhou,[34] L. P. Zhou,[1,64] S. Zhou,[6] X. Zhou,[77] X. K. Zhou,[6] X. R. Zhou,[72,58] X. Y. Zhou,[39] Y. Z. Zhou,[12,g] Z. C. Zhou,[20] A. N. Zhu,[64] J. Zhu,[43] K. Zhu,[1] K. J. Zhu,[1,58,64] K. S. Zhu,[12,g] L. Zhu,[34] L. X. Zhu,[64] S. H. Zhu,[71] T. J. Zhu,[12,g] W. D. Zhu,[41] Y. C. Zhu,[72,58] Z. A. Zhu,[1,64] J. H. Zou,[1] and J. Zu[72,58]

(BESIII Collaboration)

[1]Institute of High Energy Physics, Beijing 100049, People's Republic of China
[2]Beihang University, Beijing 100191, People's Republic of China
[3]Bochum Ruhr-University, D-44780 Bochum, Germany
[4]Budker Institute of Nuclear Physics SB RAS (BINP), Novosibirsk 630090, Russia
[5]Carnegie Mellon University, Pittsburgh, Pennsylvania 15213, USA
[6]Central China Normal University, Wuhan 430079, People's Republic of China
[7]Central South University, Changsha 410083, People's Republic of China
[8]China Center of Advanced Science and Technology, Beijing 100190, People's Republic of China
[9]China University of Geosciences, Wuhan 430074, People's Republic of China
[10]Chung-Ang University, Seoul, 06974, Republic of Korea
[11]COMSATS University Islamabad, Lahore Campus, Defence Road, Off Raiwind Road, 54000 Lahore, Pakistan
[12]Fudan University, Shanghai 200433, People's Republic of China
[13]GSI Helmholtzcentre for Heavy Ion Research GmbH, D-64291 Darmstadt, Germany
[14]Guangxi Normal University, Guilin 541004, People's Republic of China
[15]Guangxi University, Nanning 530004, People's Republic of China
[16]Hangzhou Normal University, Hangzhou 310036, People's Republic of China
[17]Hebei University, Baoding 071002, People's Republic of China
[18]Helmholtz Institute Mainz, Staudinger Weg 18, D-55099 Mainz, Germany
[19]Henan Normal University, Xinxiang 453007, People's Republic of China
[20]Henan University, Kaifeng 475004, People's Republic of China
[21]Henan University of Science and Technology, Luoyang 471003, People's Republic of China
[22]Henan University of Technology, Zhengzhou 450001, People's Republic of China
[23]Huangshan College, Huangshan 245000, People's Republic of China
[24]Hunan Normal University, Changsha 410081, People's Republic of China
[25]Hunan University, Changsha 410082, People's Republic of China
[26]Indian Institute of Technology Madras, Chennai 600036, India
[27]Indiana University, Bloomington, Indiana 47405, USA
[28a]INFN Laboratori Nazionali di Frascati, I-00044, Frascati, Italy
[28b]INFN Sezione di Perugia, I-06100, Perugia, Italy
[28c]University of Perugia, I-06100, Perugia, Italy
[29a]INFN Sezione di Ferrara, I-44122, Ferrara, Italy
[29b]University of Ferrara, I-44122, Ferrara, Italy
[30]Inner Mongolia University, Hohhot 010021, People's Republic of China
[31]Institute of Modern Physics, Lanzhou 730000, People's Republic of China
[32]Institute of Physics and Technology, Peace Avenue 54B, Ulaanbaatar 13330, Mongolia
[33]Instituto de Alta Investigación, Universidad de Tarapacá, Casilla 7D, Arica 1000000, Chile
[34]Jilin University, Changchun 130012, People's Republic of China
[35]Johannes Gutenberg University of Mainz, Johann-Joachim-Becher-Weg 45, D-55099 Mainz, Germany
[36]Joint Institute for Nuclear Research, 141980 Dubna, Moscow region, Russia
[37]Justus-Liebig-Universitaet Giessen, II. Physikalisches Institut, Heinrich-Buff-Ring 16, D-35392 Giessen, Germany
[38]Lanzhou University, Lanzhou 730000, People's Republic of China
[39]Liaoning Normal University, Dalian 116029, People's Republic of China
[40]Liaoning University, Shenyang 110036, People's Republic of China
[41]Nanjing Normal University, Nanjing 210023, People's Republic of China
[42]Nanjing University, Nanjing 210093, People's Republic of China
[43]Nankai University, Tianjin 300071, People's Republic of China
[44]National Centre for Nuclear Research, Warsaw 02-093, Poland
[45]North China Electric Power University, Beijing 102206, People's Republic of China
[46]Peking University, Beijing 100871, People's Republic of China
[47]Qufu Normal University, Qufu 273165, People's Republic of China
[48]Renmin University of China, Beijing 100872, People's Republic of China
[49]Shandong Normal University, Jinan 250014, People's Republic of China
[50]Shandong University, Jinan 250100, People's Republic of China
[51]Shanghai Jiao Tong University, Shanghai 200240, People's Republic of China
[52]Shanxi Normal University, Linfen 041004, People's Republic of China
[53]Shanxi University, Taiyuan 030006, People's Republic of China
[54]Sichuan University, Chengdu 610064, People's Republic of China

[55]Soochow University, Suzhou 215006, People's Republic of China
[56]South China Normal University, Guangzhou 510006, People's Republic of China
[57]Southeast University, Nanjing 211100, People's Republic of China
[58]State Key Laboratory of Particle Detection and Electronics, Beijing 100049, Hefei 230026, People's Republic of China
[59]Sun Yat-Sen University, Guangzhou 510275, People's Republic of China
[60]Suranaree University of Technology, University Avenue 111, Nakhon Ratchasima 30000, Thailand
[61]Tsinghua University, Beijing 100084, People's Republic of China
[62a]Turkish Accelerator Center Particle Factory Group, Istinye University, 34010, Istanbul, Turkey
[62b]Near East University, Nicosia, North Cyprus, 99138, Mersin 10, Turkey
[63]University of Bristol, H H Wills Physics Laboratory, Tyndall Avenue, Bristol BS8 1TL, United Kingdom
[64]University of Chinese Academy of Sciences, Beijing 100049, People's Republic of China
[65]University of Groningen, NL-9747 AA Groningen, The Netherlands
[66]University of Hawaii, Honolulu, Hawaii 96822, USA
[67]University of Jinan, Jinan 250022, People's Republic of China
[68]University of Manchester, Oxford Road, Manchester, M13 9PL, United Kingdom
[69]University of Muenster, Wilhelm-Klemm-Strasse 9, 48149 Muenster, Germany
[70]University of Oxford, Keble Road, Oxford OX13RH, United Kingdom
[71]University of Science and Technology Liaoning, Anshan 114051, People's Republic of China
[72]University of Science and Technology of China, Hefei 230026, People's Republic of China
[73]University of South China, Hengyang 421001, People's Republic of China
[74]University of the Punjab, Lahore-54590, Pakistan
[75a]University of Turin and INFN, I-10125, Turin, Italy
[75b]University of Eastern Piedmont, I-15121, Alessandria, Italy
[75c]INFN, I-10125, Turin, Italy
[76]Uppsala University, Box 516, SE-75120 Uppsala, Sweden
[77]Wuhan University, Wuhan 430072, People's Republic of China
[78]Yantai University, Yantai 264005, People's Republic of China
[79]Yunnan University, Kunming 650500, People's Republic of China
[80]Zhejiang University, Hangzhou 310027, People's Republic of China
[81]Zhengzhou University, Zhengzhou 450001, People's Republic of China

[a]Deceased.
[b]Also at the Moscow Institute of Physics and Technology, Moscow 141700, Russia.
[c]Also at the Novosibirsk State University, Novosibirsk, 630090, Russia.
[d]Also at the NRC "Kurchatov Institute," PNPI, 188300, Gatchina, Russia.
[e]Also at Goethe University Frankfurt, 60323 Frankfurt am Main, Germany.
[f]Also at Key Laboratory for Particle Physics, Astrophysics and Cosmology, Ministry of Education; Shanghai Key Laboratory for Particle Physics and Cosmology; Institute of Nuclear and Particle Physics, Shanghai 200240, People's Republic of China.
[g]Also at Key Laboratory of Nuclear Physics and Ion-beam Application (MOE) and Institute of Modern Physics, Fudan University, Shanghai 200443, People's Republic of China.
[h]Also at State Key Laboratory of Nuclear Physics and Technology, Peking University, Beijing 100871, People's Republic of China.
[i]Also at School of Physics and Electronics, Hunan University, Changsha 410082, China.
[j]Also at Guangdong Provincial Key Laboratory of Nuclear Science, Institute of Quantum Matter, South China Normal University, Guangzhou 510006, China.
[k]Also at MOE Frontiers Science Center for Rare Isotopes, Lanzhou University, Lanzhou 730000, People's Republic of China.
[l]Also at Lanzhou Center for Theoretical Physics, Lanzhou University, Lanzhou 730000, People's Republic of China.
[m]Also at the Department of Mathematical Sciences, IBA, Karachi 75270, Pakistan.
[n]Also at Ecole Polytechnique Federale de Lausanne (EPFL), CH-1015 Lausanne, Switzerland.
[o]Also at Helmholtz Institute Mainz, Staudinger Weg 18, D-55099 Mainz, Germany.
[p]Also at School of Physics, Beihang University, Beijing 100191, China.